



0021-8502(94)00131-6

## PERFORMANCE ASSESSMENT OF THREE PERSONAL CYCLONE MODELS, USING AN AERODYNAMIC PARTICLE SIZER

A. D. Maynard and L. C. Kenny

The Health and Safety Laboratory, Health and Safety Executive, Broad Lane, Sheffield S3 7HQ, U.K.

(First received 2 June 1994; and in final form 26 September 1994)

**Abstract**—The sampling efficiency of three types of personal cyclone has been experimentally measured at a sampling flow rate of  $2.1 \text{ l min}^{-1}$ . All samplers were based on the original Higgins and Dewell-type cyclone. Samplers were characterised using a polydisperse glass microsphere aerosol contained in a calm air chamber. A modified Aerodynamic Particle Sizer was used to determine the particle size distribution of the aerosol entering and leaving the cyclones. Two of the cyclone types were shown to be statistically identical within experimental errors, when characterised in terms of their  $d_{50}$  points. However, the third type showed a significant deviation in sampling characteristics from the others. It was possible to trace this to a manufacturing error, which has since been rectified. Comparison with previously measured cyclone efficiency curves using similar techniques was good, indicating that characterising aerosols samplers using the APS and polydisperse aerosols is at a stage where experimental errors are not dominated by the instrument, or the aerosol type.

### 1. INTRODUCTION

Sampling devices for aerosol particles are usually designed to have a uniform sampling efficiency over a specified range of particle sizes. However, for health-related sampling, for example, in occupational hygiene, it is more important to sample with the same efficiency as the relevant part of the respiratory system. To this end, target sampling conventions have been defined for three regions: respirable (for aerosol exposure to the alveolar region of the lungs), thoracic (exposure below the head airways) and inhalable (exposure throughout the respiratory system) (CEN, 1993).

When taking biologically relevant samples, there is therefore a need to ensure the sampler follows the correct convention to within well-defined performance criteria. In the past this has largely been carried out by measuring sampling efficiency at a number of discrete particle sizes, using monodisperse aerosols. Such experiments are costly and time intensive. An alternative approach that has been used in recent years (e.g. Lidén and Kenny, 1991) involves using a polydisperse aerosol, effectively allowing sampler efficiency to be measured over a wide number of particle diameters simultaneously. Such an approach can be seen to be less costly and time intensive than testing with monodisperse aerosols.

Carrying out sampler efficiency tests with a polydisperse aerosol requires being able to count and size particles both in the collected sample, and in the ambient aerosol. This may be achieved by using techniques such as Coulter analysis on sampled aerosol. Quicker results may be achieved using a real time particle counter and sizer such as an optical particle detector. One instrument in particular that is used extensively for particle sizing in the range  $0.5\text{--}30 \mu\text{m}$  is the Aerodynamic Particle Sizer (APS), manufactured by TSI Incorporated, U.S.A.

As understanding of the operation of the APS has advanced, its use in characterising aerosol samplers has become more credible. Recent studies have used the instrument to measure the sampling efficiency of personal cyclones (Kenny and Lidén, 1991; Bartley *et al.*, 1994). The research presented here continues this work by using the APS to characterise three types of personal cyclone. This paper discusses the development and application of APS operating procedures that ensure accurate and reproducible measurements of sampler efficiency.

## 2. PERSONAL CYCLONES

### 2.1. Sampler types

Over the years, a number of cyclones based on the same design (Higgins and Dewell, 1967) have been commercially available. These have been, and still are used predominantly in the U.K. for taking respirable samples. However, there have been small variations from the original design, and the effect of these on performance has never been thoroughly investigated. The main sampler based on this design used in the U.K. is the metal bodied cyclone manufactured by Casella Ltd, U.K. Recently, a conductive plastic bodied cyclone based on the same design has become available from the same company. A third cyclone type based on the original Higgins and Dewell design is manufactured in the U.S.A. by BGI Inc. These were the three cyclone types tested.

For agreement with the BMRC respirable convention, cyclones based on the Higgins and Dewell design are used at a flow rate of  $1.9 \text{ l min}^{-1}$ . However, Lidén and Kenny (1993) have suggested that sampling at  $2.1 \text{ l min}^{-1}$  will lead to better agreement with the ISO/CEN/ACGIH respirable sampling convention (CEN, 1993). This was therefore the flow rate used in all tests.

### 2.2. Sampling efficiency definition

The overall sampling efficiency of a cyclone,  $E_{\text{cyclone}}$ , can be subdivided into three individual components: the efficiency with which particles are sampled by the inlet,  $E_{\text{aspiration}}$ , the transfer efficiency within the body of the cyclone,  $E_{\text{body}}$ , and the transfer efficiency between the vortex finder and the filter,  $E_{\text{finder}}$ .  $E_{\text{cyclone}}$  is then given by

$$E_{\text{cyclone}} = E_{\text{aspiration}} \cdot E_{\text{body}} \cdot E_{\text{finder}}. \quad (1)$$

Each transfer efficiency is defined as the ratio of the particle number density leaving a section ( $n_{\text{out}}$ ) to the particle number density entering the section ( $n_{\text{in}}$ ), as a function of particle aerodynamic diameter ( $d_{\text{ae}}$ ):

$$E(d_{\text{ae}}) = \frac{n_{\text{out}}(d_{\text{ae}})}{n_{\text{in}}(d_{\text{ae}})}. \quad (2)$$

By operating the cyclones under calm air conditions, the Agarwal-Liu calm air criteria was met for particles of aerodynamic diameter  $< 38 \mu\text{m}$  (Agarwal and Liu, 1980). For sampling an aerosol with particles up to  $d_{\text{ae}} = 10 \mu\text{m}$  using a 4 mm inside diameter tube (equivalent to the cyclone inlet), it has been estimated that air velocities lower than  $0.5 \text{ m s}^{-1}$  constitute calm air conditions (Vincent, 1989). Measurements were carried out at air velocities of approximately  $1 \text{ mm s}^{-1}$ , thus allowing the assumption that  $E_{\text{aspiration}} \sim 1$ .

$E_{\text{finder}}$  was assumed to be the same as the transfer efficiency from the vortex finder to the sampling system. Thus, overall sampling efficiency was measured by comparing the ratio of the aerosol concentration sampled directly after the vortex finder ( $n_{\text{out}}(d_{\text{ae}})$ ), to the ambient aerosol concentration ( $n_{\text{in}}(d_{\text{ae}})$ ).

### 2.3. Calculation of cyclone sampling efficiency

Measurement of both  $n_{\text{in}}$  and  $n_{\text{out}}$  was carried out by using an APS remote from the sampling point. The actual particle number concentration measured by the device ( $n'(d_{\text{ae}})$ ) was therefore influenced by the transfer efficiency of the tube from the sampling point to the APS inlet ( $E_{\text{tube}}$ ):

$$n'(d_{\text{ae}}) = n(d_{\text{ae}}) \cdot E_{\text{tube}}(d_{\text{ae}}). \quad (3)$$

If  $E_{\text{tube}}$  is constant in all measurements, equation (3) may be used to derive  $n(d_{\text{ae}})$ . Additionally, substitution of equation (3) into equation (2) shows measured cyclone efficiency to be independent of  $E_{\text{tube}}$ , allowing  $E_{\text{cyclone}}$  to be calculated directly from the measured

particle concentration. The assumption that  $E_{\text{tube}}$  is constant for all measurements was taken to be valid in this study, although there is the possibility of turbulent flow from the cyclone vortex finder outlet leading to increased particle deposition.

The analytical technique used to measure particle concentration and size distribution limited measurements to being taken serially, resulting in  $n_{\text{in}}$  and  $n_{\text{out}}$  being measured in sequence. To average out possible time variations in the ambient aerosol particle concentration, each cyclone efficiency test consisted of a series of measurements:  $n_{\text{in}}^1, n_{\text{out}}^1, n_{\text{in}}^2, n_{\text{out}}^2, n_{\text{in}}^3$ . Measurements were averaged to give  $\bar{n}_{\text{in}}$  and  $\bar{n}_{\text{out}}$ .

Possible differences between  $\bar{n}_{\text{in}}$  and  $\bar{n}_{\text{out}}$  attributable to time variations in the total ambient aerosol concentration, were overcome by normalising  $\bar{n}_{\text{in}}$  to give  $E = 1$  at small particle diameters (e.g. Iles, 1990). In this way, the ambient aerosol was only required to be stable with respect to relative particle concentration, as a function of  $d_{\text{ae}}$ . From initial tests, it was confirmed that the cyclone efficiency could be considered as constant between 1.5 and 2.3  $\mu\text{m}$ . It was therefore assumed that sampling efficiency was 100% in this region. The normalisation constant was calculated by summing the ratio of particle concentrations for each discrete measured particle size between these limits:

$$E_{\text{body}}(d_{\text{ae}}) = \frac{\bar{n}_{\text{out}}(d_{\text{ae}})}{\bar{n}_{\text{in}}(d_{\text{ae}})} \cdot \frac{1}{N} \sum_{d_{\text{ae}}=1.5}^{2.3} \frac{n_{\text{in}}(d_{\text{ae}})}{n_{\text{out}}(d_{\text{ae}})}, \quad (4)$$

where

$$\bar{n}_{\text{in}}(d_{\text{ae}}) = \frac{1}{3} \sum_{a=1}^3 n_{\text{in}}^a(d_{\text{ae}}) \quad \text{and} \quad \bar{n}_{\text{out}}(d_{\text{ae}}) = \frac{1}{2} \sum_{a=1}^2 n_{\text{out}}^a(d_{\text{ae}}),$$

and  $N$  is the number of discrete particle diameters summed over.

### 3. EXPERIMENTAL DETAILS

#### 3.1. Test aerosol generation

The aerosol used for measuring cyclone efficiency was a dispersed Whitehouse Scientific glass microsphere dust (GS 5000, nominal mass distribution 2.5–20  $\mu\text{m}$ ). The density of the powder was measured, and found to be within 0.5% of the manufacturers stated density of 2.45  $\text{g cm}^{-3}$ . This value was used for carrying out particle density correction on the APS data (Wang and John, 1987). Dispersion was achieved using a Rotating Brush Generator (RBG) manufactured by PALAS, Germany. The aerosol was passed over a  $\text{Kr}^{85}$  source before entering the calm air chamber to bring it to charge equilibrium.

The RBG was operated at a dust volume feed rate of 20  $\text{mm}^3 \text{h}^{-1}$  (1  $\text{mm h}^{-1}$  of a 5 mm diameter compacted dust column), with a brush rotation of 1188 rpm and an air flow of 25  $\text{l min}^{-1}$ . The detected ambient particle concentration produced was between 80 and 100 particles  $\text{cm}^{-3}$ .

#### 3.2. Calm air chamber

Aerosol generated by the RBG was fed at a constant rate to the top of the calm air dust chamber throughout the experiment. This consisted of three sections: a mixing chamber, a sampling chamber and an extraction chamber (Fig. 1). All were sealed to the external atmosphere, bar the inlets and outlets. The top and bottom sections were separated from the sampling chamber by aluminium "honeycomb" to minimise turbulence. Aerosol mixing in the top chamber was achieved by a slowly rotating rotor (running at approximately 30 rpm). Air was extracted from the bottom section of the chamber at 60  $\text{l min}^{-1}$ . The sampling chamber was 1  $\text{m}^2$  in cross-sectional area, leading to an average downwards air velocity of 1  $\text{mm s}^{-1}$ , thus ensuring all sampling was well within calm air conditions. The additional air required to make up the 60  $\text{l min}^{-1}$  through-flow was drawn into the calm air chamber via a HEPA filter, entering in an annulus around the aerosol inlet. The resulting pressure drop in the chamber relative to ambient conditions was  $\sim 2 \text{ mmHg}_2\text{O}$ .

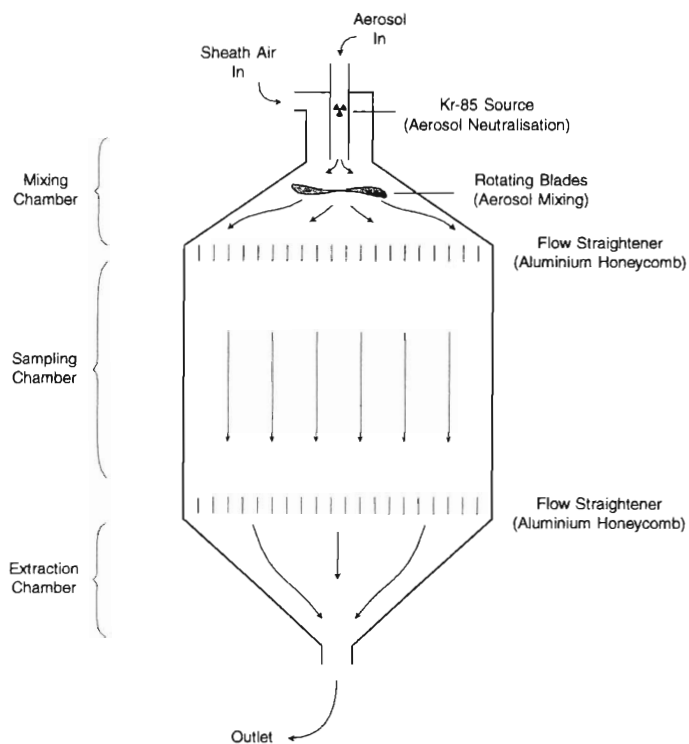


Fig. 1. Schematic of the calm air chamber used in testing cyclone sampling efficiency.

Investigations showed that the aerosol number concentration in the sampling chamber stabilised after about 1 h. The chamber was therefore allowed to reach equilibrium for at least this length of time before each series of tests.

### 3.3. APS set-up and use

**3.3.1. APS position.** Placing the APS in the calm air chamber was found to disrupt highly the flow field, and the aerosol concentration stability. It was therefore positioned outside the chamber, with a sampling tube leading from its inlet to the cyclone test position (which was about 30 cm from the centre, and 20 cm from the base of the chamber). The sampling tube was 10 mm inside diameter, with a horizontal length of 476 mm and two 90° bends. These dimensions were designed to give it a maximum transmittance between 1 and 10  $\mu\text{m}$ .

**3.3.2. Cyclone attachment.** Under standard operating conditions, the APS samples at a flow rate of 5  $\text{l min}^{-1}$ . Although it may be used successfully at different sampling rates (Rader *et al.*, 1990), this requires substantial data manipulation outside the TSI operating software to calculate particle diameters. Previous work using the APS with samplers operating at less than 5  $\text{l min}^{-1}$  has overcome the problem by supplying extra air flow to the instrument after the sampler (Kenny and Lidén, 1991).

Air entering the APS is divided into two flows in the ratio 4:1. The lower flow rate constitutes the sample flow, and passes directly into the sensing chamber. The remaining flow is filtered, and recombined with the sample flow as an annular sheath flow. By disconnecting the sheath flow from the APS inlet, it was modified to allow sampling rates as low as 1  $\text{l min}^{-1}$  under standard operating conditions (Fig. 2). An external sampling pump was used to draw extra "makeup flow" through the inlet to make the sampling rate up to the required value (2.1  $\text{l min}^{-1}$ ). The 4  $\text{l min}^{-1}$  sheath flow into the APS sensing zone was drawn in from the laboratory air. Cyclone sampling rate was set using a Gillibrator™ bubble flow meter (Gillian Instrument Corp., U.S.A.) before each set of measurements.

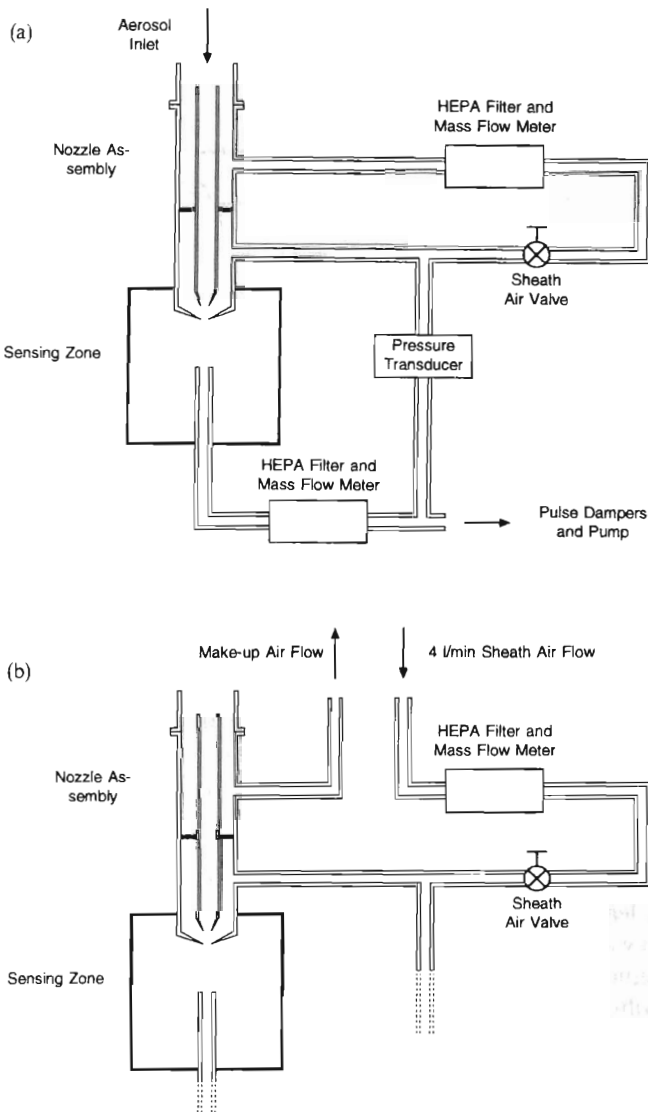


Fig. 2. Schematic of the APS sampling system: (a) before modification; (b) after modification. The sheath flow inlet was disconnected from the APS inlet, allowing a minimum sampling rate of  $1 \text{ l min}^{-1}$ . By drawing make-up air through the former sheath flow inlet, the sampling rate was increased to  $2.1 \text{ l min}^{-1}$ ;  $4 \text{ l min}^{-1}$  sheath air was drawn into the APS from the laboratory.

Cyclones were attached to the extended APS inlet in such a way as to allow the vortex finder to lead directly into the inlet extension, thus effectively eliminating the effects of  $E_{\text{finder}}$ . The attachment method for each of the cyclones tested is shown in Fig. 3. All attachments were leak-tight. Differences in measured efficiency due to the attachment method were assumed to be negligible. Losses in the sampling tube due to turbulence from the vortex finder were also assumed to be negligible.

**3.3.3. Validation of the APS calibration.** The relationship between particle time-of-flight and aerodynamic diameter in the APS is highly dependent on operating conditions, leading to a need to validate the calibration function before taking readings. In this series of experiments, the APS calibration was checked before use with certified monodisperse polystyrene latex spheres (traceable to National Institute of Standards and Technology (NIST), and Community Bureau of Reference (BCR) standards). These were prepared by

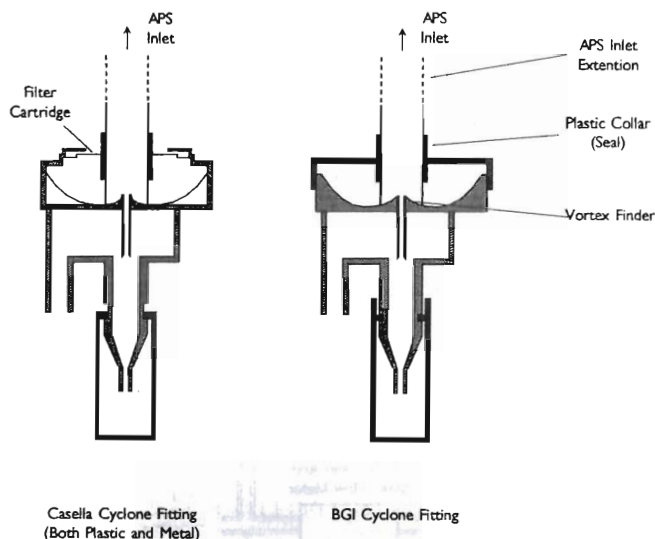


Fig. 3. Schematics of the Casella and BGI cyclones, showing the method of attachment to the APS extension inlet.

placing a few drops of iso-propyl alcohol (IPA) on a clean glass microscope slide, and then adding a drop of dispersed latex particle suspension. Mixing the suspension and IPA together on the slide, then allowing the liquid to evaporate, gave a relatively uniform coating of particles. These could subsequently be brushed into the APS inlet as discrete particles, using a fine artists brush. This preparation technique does not altogether prevent surfactant within the particle suspension drying as a shell round the particles, although diluting with IPA leads to this layer having a negligible effect on particle size.

APS calibration was verified at three particle sizes (2, 5 and 7  $\mu\text{m}$ ), covering the transition region from high efficiency to low efficiency in the cyclone. On most occasions it was found that calibration drifted from day to day. The APS was therefore brought back to calibration by setting the pressure drop across the nozzles to the factory calibration value, and altering the sheath flow until the reference latex spheres were sampled with the correct time-of-flight. Although this technique does not fully compensate for drifts in calibration, it gives a sufficient approximation where laboratory conditions are not dissimilar to the factory calibration conditions. Resulting variations in calibration at the test particle diameters were smaller than the error within the APS calibration function.

3.3.4. *Coincidence correction in the APS.* In common with other particle counting and sizing devices that rely on optical sensing, the APS is prone to particle coincidence errors. The nature of these errors is well documented (e.g. Baron *et al.*, 1993; Heitbrink and Baron, 1992).

The problem of coincidence tends to be exacerbated when there are a large number of particles around the detection limit of the APS present in the sampled aerosol. This leads to the generation of "phantom particles" which are random in size, leading to a uniform particle background at all diameters (Heitbrink and Baron, 1992). Phantom particle creation was found to be a significant problem with the polydisperse glass microsphere powder used in this experiment.

To reduce the level of coincidence from submicron particles, the sensitivity of the pulse formation system in the APS was reduced by lowering the photomultiplier tube sensitivity (TSI, 1987). One consequence of this was the imperfect detection of particles with diameters above the lower detection limit, due to Mie scattering (see Rader and O'Hern, 1993), resulting in spurious notches in the particle size distribution (a prominent notch occurs at  $\sim 2.5 \mu\text{m}$ ). As relative changes in particle concentration were being considered when

measuring cyclone performance, it was assumed that this feature would have no bearing on the final calculated efficiency.

A further consequence of altering the photomultiplier tube sensitivity is that detected pulse heights do not correspond with preset particle selection criteria in the APS. The effects of this are more severe for particles of aerodynamic diameter above  $15\ \mu\text{m}$ , which are processed by a separate processor within the instrument (the large particle processor). Therefore, only particle size data up to  $15\ \mu\text{m}$  was used in this case (using the output of the APS's small particle processor).

To correct for remaining phantom errors prior to calculating sampler efficiency, it was assumed that cyclone efficiency fell to zero at large particle diameters. Following this assumption, the average value of  $\bar{n}_{\text{out}}(d_{\text{ae}})$  as measured by the APS at large particle diameters should represent the average phantom particle level. Investigation of  $\bar{n}_{\text{out}}$  for a cyclone measured by the APS indicated it to be approximately constant above  $10\ \mu\text{m}$ , when sampling at  $2.1\ \text{l min}^{-1}$ . Thus, the average coincidence level  $\bar{n}_c$  was obtained by averaging  $\bar{n}_{\text{out}}$  at all diameters above  $10\ \mu\text{m}$ :

$$\bar{n}_c = \sum_{d_{\text{ae}}=10\ \mu\text{m}}^{15\ \mu\text{m}} \frac{n_{\text{out}}(d_{\text{ae}})}{N}, \quad (5)$$

where  $N$  is the number of discrete particle diameters summed over;  $\bar{n}_c$  was then subtracted from  $\bar{n}_{\text{out}}$ . It was also assumed to be a good estimate for the coincidence level in  $\bar{n}_{\text{in}}$  after normalisation, as at small diameters the number concentrations entering the APS should have been similar.

The average coincidence level was typically of the order of  $0.003\ \text{particles cm}^{-3}\ \mu\text{m}^{-1}$ , corresponding to around 0.1% of  $\bar{n}_{\text{out}}$  at  $2\ \mu\text{m}$ , and 1% of  $\bar{n}_{\text{out}}$  at  $5\ \mu\text{m}$ .

### 3.5. Experimental design

Two specimens of each cyclone type were selected for testing, giving six specimens in all. Each specimen was tested six times, with all cyclones randomly distributed through the testing sequence. Each test consisted of alternately sampling the ambient aerosol, then the cyclone output, in sequence. The ambient aerosol was sampled three times, and initiated and terminated the test sequence; aerosol exiting the cyclone vortex finder was sampled twice in each sequence. Each sample was acquired for 60 s (active APS time). The time taken to set each sample up lead to the total time for each test being approximately 10 min. The tests were carried out over a continuous time period, with the APS calibration being checked before and after all cyclones had been tested. Cyclone sampling flow rate was also measured at the beginning and end of the sequence, using a Gillibrator<sup>TM</sup> bubble flow meter.

## 4. RESULTS

### 4.1. Aerosol size distribution stability

The data reduction technique used to calculate cyclone efficiency relied on the relative ambient aerosol size distribution remaining constant over the time taken to test one cyclone. This was verified by examining normalised number concentration residuals,  $R$ , of the ambient aerosol, from the mean normalised particle concentration for each test,  $\bar{n}_{\text{in}}^b$ . For ambient aerosol sample  $a$ , in test  $b$ ,

$$R^{a,b}(d) = \bar{n}_{\text{in}}^b(d_{\text{ae}}) - \frac{n_{\text{in}}^{a,b}(d_{\text{ae}})}{N^{a,b}}, \quad (6)$$

where

$$\bar{n}_{\text{in}}^b(d_{\text{ae}}) = \frac{1}{3} \sum_{a=1}^3 \frac{n_{\text{in}}^{a,b}(d_{\text{ae}})}{N^{a,b}} \quad \text{and} \quad N^{a,b} = \sum_{\text{all } d_{\text{ae}}} n_{\text{in}}^{a,b}(d_{\text{ae}}).$$

Normalising  $R$  to the total particle number count in each sample allowed comparison of

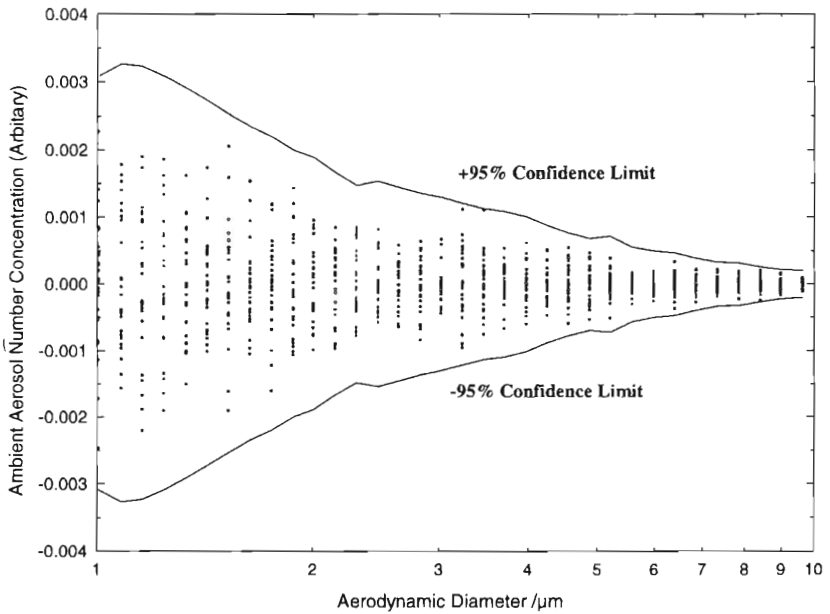


Fig. 4. Ambient aerosol number concentration residuals from mean concentration (normalised) during testing of all six cyclone samples. The  $\pm 95\%$  confidence limits have been calculated from Poisson count errors associated with the mean particle concentration.

residuals from different tests. Figure 4 plots  $R$  for all samples in relation to the 95% confidence limits estimated from Poisson count errors. Values of  $R$  within these limits may be assumed to be due to random count variations.

#### 4.2. Cyclone efficiency testing

Table 1 gives the  $d_{50}$  diameters for each cyclone tested, calculated by linear interpolation. Mean values and 95% confidence limits are also given. Averaged data for the cyclones are presented in Fig. 5. Duplicate efficiency data collected for one of the cyclone types one month after the original tests gave the same values of  $d_{50}$  to within  $\pm 0.05 \mu\text{m}$ .

#### 4.3. Errors

Random errors in the cyclone efficiency curves due to sampling flow variations, particle number density variations, Poisson counting errors and coincidence in the APS, were assumed to be reflected in the variance in  $d_{50}$  values for each cyclone specimen. These were typically of the order of  $\pm 2\%$  ( $\pm 2\sigma$ ).

Possible systematic errors were assumed to arise from the APS calibration, and particle density correction.

Table 1. Values of cyclone  $d_{50}$ , obtained via linear interpolation (Cyclones: CM, Casella Metal; CP, Casella Plastic; BGI, BGI Inc. Metal)

Cyclone	Run number and $d_{50}$ ( $\mu\text{m}$ )						$\bar{d}_{50}$	$\pm 95\%$ confidence limits	
	1	2	3	4	5	6			
CM1	4.957	4.968	5.029	4.985	5.003	4.897	4.973	4.926	5.020
CM2	5.073	5.116	5.111	5.140	5.220	5.083	5.124	5.068	5.180
CP 1	4.526	4.669	4.623	4.673	4.604	4.691	4.631	4.567	4.695
CP 2	4.572	4.534	4.570	4.584	4.617	4.585	4.577	4.549	4.605
BGI 1	4.655	4.529	4.566	4.504	4.568	4.572	4.566	4.512	4.620
BGI 2	4.576	4.613	4.554	4.591	4.599	4.593	4.588	4.567	4.609

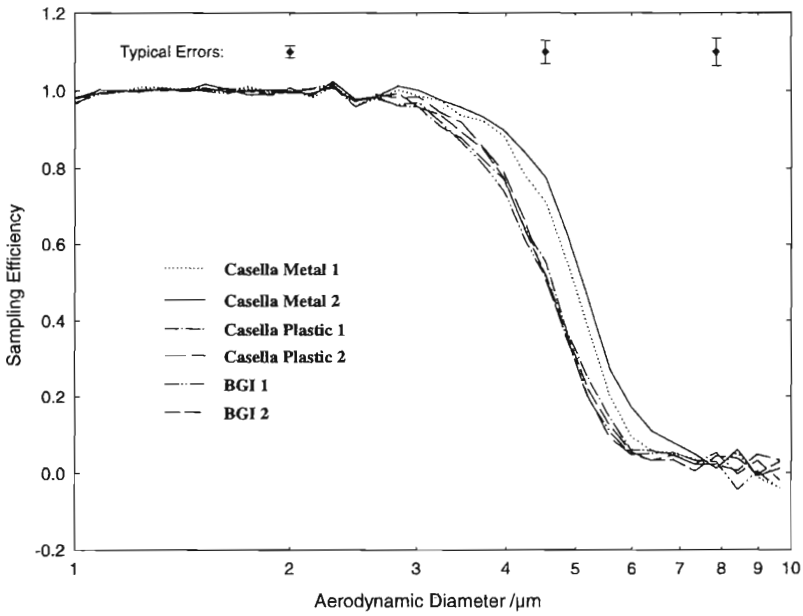


Fig. 5. Measured cyclone sampling efficiency at  $2.1 \text{ l min}^{-1}$  for each cyclone specimen. The error bars indicate the inter-run variation in penetration at 2.00, 4.54 and  $7.87 \mu\text{m}$  (as  $\pm \sigma$ ), averaged over all cyclones.

*APS calibration:* Before each test sequence, the APS was adjusted to be calibrated correctly for  $2 \mu\text{m}$  latex spheres. This led to an estimated systematic deviation from the factory calibration curve of less than 1% at  $5 \mu\text{m}$ . As this was judged to be comparable to the precision of aerodynamic diameters derived using the factory calibration, it was ignored.

*Particle density correction:* The density of the glass microspheres was measured, and found to agree with the manufacturer's value of  $2.45 \text{ g cm}^{-3}$  to within 0.5%. The corresponding shift in particle aerodynamic diameter after density correction was less than 0.05% at  $5 \mu\text{m}$ . As this was considerably smaller than the experimental error, it was considered negligible. Variations in particle density with respect to diameter have been reported in glass microsphere powders (Ball *et al.*, 1989). However, the measurements made were not sufficiently quantitative to allow size selective density correction in this experiment.

The density correction algorithm used has been estimated as giving up to a 1% systematic error (negative in this case) (Wang and John, 1987). As this is indeterminate, it was not accounted for in the data analysis.

## 5. ANALYSIS

### 5.1. Aerosol size distribution stability

Figure 4 shows particle number concentration residuals to vary randomly about zero, with the majority lying within the  $\pm 95\%$  confidence limits of a Poisson distribution. This suggests that short-term variations in number concentration were within those expected due to random errors. Any systematic errors in measuring cyclone sampling efficiency due to serial acquisition of  $n_{\text{in}}$  and  $n_{\text{out}}$  may therefore be considered insignificant.

### 5.2. Inter-specimen and inter-sampler variation

Figure 5 clearly shows that the sampling characteristics of the BGI and the Casella plastic cyclones are similar, while those of the Casella metal cyclones tested are significantly different. To examine quantitatively the equivalence of the two specimens of a given cyclone type, a two-tailed statistical test was carried out on the interpolated  $d_{50}$  values, with

Table 2. Results of a two-tailed *t*-test on cyclones of the same type (Cyclones: CM, Casella Metal; CP, Casella Plastic; BGI: BGI Inc. Metal)

Sampler type	$\bar{d}_{50}^1$	$\bar{d}_{50}^2$	$\bar{d}_{50}$	Estimated $\sigma$	Degress of freedom	<i>t</i> -statistic	Significance level
CM	4.973	5.124	5.049	0.049	10	- 5.320	< 0.05%
CP	4.631	4.577	4.604	0.047	10	1.983	> 2.5%
BGI	4.566	4.588	4.577	0.039	10	- 1.704	> 5%

Table 3. Results of a two-tailed *t*-test on cyclones of different types

Sampler types	$\bar{d}_{50}^1$	$\bar{d}_{50}^2$	Degrees of freedom	<i>t</i> -statistic	Significance level
Casella Metal & Casella Plastic	5.049	4.604	22	- 18.542	<< 0.05%
Casella Metal & BGI	5.049	4.577	22	21.317	<< 0.05%
Casella Plastic & BGI	4.604	4.577	22	1.219	> 10%

$\bar{d}_{50} = \bar{d}_{50}^2$  as the null hypothesis. Table 2 gives the results of the test as applied to interpolated  $\bar{d}_{50}$  values from each cyclone specimen. The values of the *t*-statistic indicate the inter-specimen variation. The BGI cyclones agree to within a 5% significance level, while the Casella plastic cyclones lie just outside this. However, the inter-specimen variation of the Casella metal cyclone is more than an order of magnitude worse.

For two sampler types to be considered statistically identical, the inter-sampler variation should be comparable with inter-specimen variation, using the same null hypothesis as before. Table 3 gives the results of two-tailed tests between different sampler types. It clearly shows that while the BGI and Casella plastic cyclones may be considered identical in terms of their  $\bar{d}_{50}$  values from this test, the Casella metal cyclones are significantly different from either of the other types.

From discussion with Casella Ltd, it was found that a machining error had led to the cyclone inlet slots being 13% wider than the accepted dimension. Acceptable tolerance limits had been set at  $\pm 3\%$ . The inlet slots were subsequently modified, giving the same area as cyclones built to within tolerance limits: subsequent sampling efficiency tests carried out on these cyclones showed closer agreement with the Casella plastic and BGI cyclones. Further evidence from pre-1986 metal Casella cyclones made to within tolerance limits (Lidén and Kenny, 1991) indicated that the change in inlet slot width was predominantly responsible for the shift in sampling efficiency. This problem has since been rectified.

### 5.3. Measured cyclone efficiency

5.3.1. *Anomalies in the efficiency curve shape.* Referring back to Fig. 5, all cyclones appear to show a small decrease in efficiency at  $\sim 1 \mu\text{m}$ , and a dip in efficiency at  $\sim 2.5 \mu\text{m}$ . While these features do not have any direct bearing on the main efficiency characteristics between  $\sim 3$  and  $7 \mu\text{m}$ , they nonetheless represent a departure from the expected behaviour. The question of whether they are real effects, or artefacts of the APS or the subsequent data processing, must therefore be considered.

The probability of the features being a real attribute of cyclone sampling efficiency is exceptionally low: no such features have been observed in the past, there is no theoretical model that would explain them, and there appears to be no correlation between the particle diameter the dips occur at, and the shape of individual cyclone efficiency curves.

If it is assumed that the cyclone sampling efficiency is essentially unity below  $2.5 \mu\text{m}$ , then for the features to appear on the efficiency curve, they must be introduced in the APS, or in the subsequent data processing. Assuming that the particle size distribution seen by the APS below  $2.5 \mu\text{m}$  is the same with and without the cyclone, for the features to be a direct

Table 4. Cyclone curve fitting values (Cyclones: CM, Casella Metal; CP, Casella Plastic; BGI, BGI Inc. Metal)

Cyclone	$c$	$\bar{d}_{50}(\mu\text{m})$	$\pm 95\%$ confidence limits on $\bar{d}_{50}(\mu\text{m})$	
CM1	0.496	4.958	4.923	4.993
CM2	0.532	5.145	5.113	5.176
CP1	0.556	4.610	4.579	4.642
CP2	0.515	4.531	4.506	4.556
BGI1	0.464	4.574	4.547	4.601
BGI2	0.504	4.582	4.554	4.609

result of the APS they would have to be caused by differences in concentration at larger particle sizes: no evidence is seen of this.

With the photomultiplier tube sensitivity reduced in the APS, there is a significant decrease in measured particle concentration at around  $2.5 \mu\text{m}$  due to Mie scattering. The correlation between this effect, and the feature in the efficiency curves, can be explained by the phantom particle background being lower with the cyclone on the APS inlet. This could only be caused by fewer fine particles entering the APS inlet with the cyclone present, and is hinted at in the efficiency curves around  $1 \mu\text{m}$ . However, whether the effect is due to losses within the cyclone, or losses at the vortex finder outlet, is impossible to determine from these data.

**5.3.2. Curve fitting.** Curve fitting was carried out by modelling the pooled data for a cyclone specimen from all tests in the sequence, allowing the measured efficiency to be treated as a mathematical function. This was carried out using a weighted non-linear least-squares fitting method (using the software package Tablecurve from Jandel Scientific, Germany). A sigmoid function of the form

$$E(d_{ae}) = \frac{1}{1 + \exp\left(\frac{(d_{ae} - d_{50})}{c}\right)} \quad (7)$$

was found to model the data well. Previous studies of similar cyclones have used the Blachmann–Lippmann function (Lidén and Kenny, 1991), and the cumulative log-normal function (Bartley *et al.*, 1994). Table 4 summarises the values of  $d_{50}$  obtained, as well as the confidence limits from the fit, and the fitting parameter  $c$ . The  $d_{50}$  values obtained agree well with those from linear interpolation (Table 1).

## 6. COMPARISON WITH OTHER RESULTS

Although there have been a number of studies of cyclone efficiency, it is only relatively recently that experimental techniques have become sensitive enough to allow the possibility of valid data comparisons. Therefore, the results of this study are compared against those from two of the most recent cyclone efficiency tests. These are the tests conducted by Kenny and Lidén (1991; see also Lidén and Kenny, 1991) and Bartley *et al.* (1994). A more thorough comparison of efficiency curve data will be presented in a later paper.

Kenny and Lidén carried out a series of tests on personal cyclones at different flow rates, using two different aerosols. All tests were carried out using an APS sampling an aerosol contained in a calm air chamber, in a manner similar to that used in the current experiment. The two aerosols used consisted of PVA particles, and silicone oil particles, respectively. Significant differences in efficiency curve shape and  $d_{50}$  values were noted between the two aerosols. In addition, results using PVA were shown to vary significantly when measured a year later. No additional measurements were taken with the silicone oil aerosol.

Kenny and Lidén compared their results against earlier measurements by Higgins and Dewell (1967), Maguire *et al.* (1973), Ogden *et al.* (1983) and Vaughan (1983). Large

Table 5. Comparative cyclone efficiency data at a sampling flow rate of  $2.1 \text{ l min}^{-1}$ , for SIMPEDS type cyclones

	$d_{50}(\mu\text{m})$	$c$
This study	4.5749	0.496
Lidén and Kenny (1991) PVA	4.23	0.661*
Lidén and Kenny (1991) silicone oil	4.65	0.581*
Bartley <i>et al.</i> (1993)	4.595	0.511*

\*These values have been derived from data presented by the authors (see text).

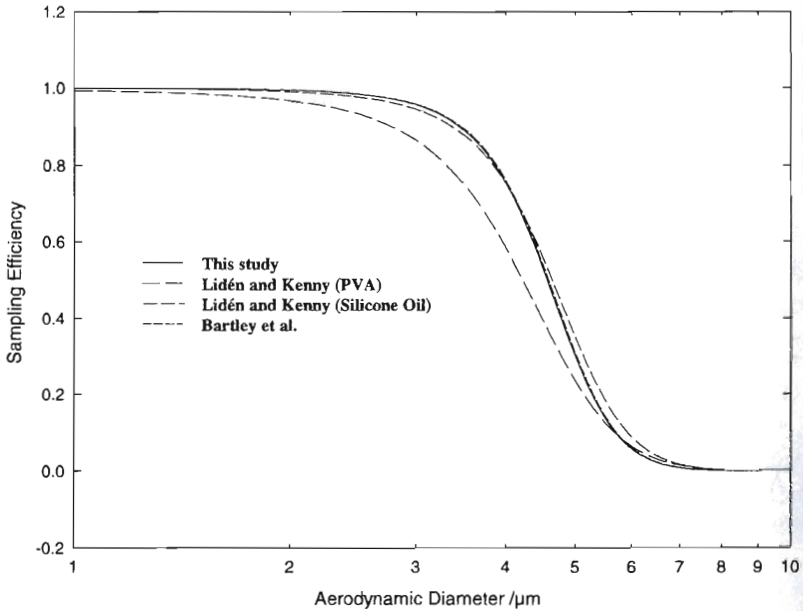


Fig. 6. Comparison of modelled cyclone sampling efficiency at  $2.1 \text{ l min}^{-1}$  from this study; Lidén and Kenny (1991) and Bartley *et al.* (1993).

variations were found both in efficiency curve shape and  $d_{50}$  values from the earlier data. However, values of  $d_{50}$  from Ogden *et al.* using a coal dust aerosol (with Coulter analysis), and from Vaughan, using a DOP aerosol with the APS, agree well with the  $d_{50}$  values of Kenny and Lidén from silicone oil (Lidén and Kenny, 1991).

Table 5 shows data from Kenny and Lidén taken at  $2.1 \text{ l min}^{-1}$  against data from this study. As they used the Blachmann–Lippmann function to model sampling efficiency, the parameter  $c$  has been derived from their results. Figure 6 plots the two curve fits. As can be seen, there is good agreement between the silicone oil results, and the present data, both in  $d_{50}$  and curve shape. The agreement is not good with the PVA data.

Bartley *et al.* (1994) have carried out a series of tests similar to those presented here, but using a polydisperse potassium sodium tartarate aerosol. The aerosol had a mass median aerodynamic diameter of  $4.0 \mu\text{m}$ , with a geometric standard deviation of 2.2, leading to particles predominantly lying in the cyclone efficiency transition region.

Data were collected over a range of flow rates. However,  $2.1 \text{ l min}^{-1}$  was not covered. The  $d_{50}$  value in Table 5 was therefore interpolated from data at  $2.0$  and  $2.5 \text{ l min}^{-1}$ . The model used for cyclone efficiency by Bartley *et al.* was the cumulative log-normal model, thus no direct comparison was possible between curve shapes from the study by Kenny and Lidén, and from this study. However, data at  $2.0 \text{ l min}^{-1}$  were modelled with a sigmoid function, and the value of  $c$  from this was used to estimate  $c$  at  $2.1 \text{ l min}^{-1}$ . Figure 6 plots the two

modelled curves at  $2.1 \text{ l min}^{-1}$ . As can be seen, there is good agreement between the efficiency curves.

## 7. CONCLUSIONS

The main aim of this experiment has been to characterise the sampling efficiency of three types of personal cyclone at  $2.1 \text{ l min}^{-1}$ . In achieving this, the work has allowed further assessment of the use of polydisperse aerosols in the testing of samplers, specifically with the TSI Aerodynamic Particle Sizer (APS). The APS was configured to allow a sampling rate of from  $1 \text{ l min}^{-1}$  to above  $5 \text{ l min}^{-1}$  to be used. In this configuration, it should be possible to characterise aerosol samplers over a range of sampling rates with particles of aerodynamic diameter in the region of  $0.5\text{--}15 \mu\text{m}$ . This could be extended to  $30 \mu\text{m}$  if the full sizing capability of the APS was used.

Three types of personal cyclone were characterised: the current version of the Casella metal bodied cyclone, along with the plastic bodied cyclone from the same company; and a cyclone based on the same design from BGI Inc. All cyclones were tested at  $2.1 \text{ l min}^{-1}$ , as this had been suggested as a possible sampling rate for agreement with the new ISO/CEN/ACGIH respirable convention. Two specimens of each cyclone type were tested, with each specimen being tested six times.

Cyclone efficiency  $d_{50}$  points were determined to  $\pm 0.1 \mu\text{m}$  ( $\pm 2\sigma$ ). This was within the experimental error expected from the APS readings. The resolution of the APS allowed the differentiation of differences in the cyclone efficiency curves around the  $d_{50}$  point. Statistical analysis of the interpolated  $d_{50}$  points showed the Casella plastic, and BGI cyclones to be identical. However, the sampling efficiency of the Casella metal cyclones was shown to have a significantly higher  $d_{50}$ : the Casella plastic and BGI cyclones had a pooled average  $d_{50}$  of  $4.59 \mu\text{m}$ , compared to  $5.05 \mu\text{m}$  for the Casella metal cyclones. This was traced with the help of Casella to a tolerance error of 13% on the cyclone input slot width. The problem has since been rectified.

Initial comparisons with cyclone efficiency data from Lidén and Kenny (1991) and Bartley *et al.* (1994) indicate very close agreement. These two sets of experiments used the APS in different configurations, with different polydisperse aerosols. The results therefore indicate that experimental techniques for characterising aerosols samplers using the APS and polydisperse aerosols, have developed to the point where experimental errors are small enough to allow differences between individual sampler specimens to be quantified.

*Acknowledgements*—This paper presents work supported by the Health Policy Division of the Health and Safety Executive. Thanks to R. Gussman of BGI Inc. for supplying cyclone specimens, and M. Whelan of Casella Ltd for supplying information on the metal cyclone.

## REFERENCES

- Agarwal, J. K. and Liu, B. Y. H. (1980) A criterion for accurate aerosol sampling in calm air. *Am. Ind. Hyg. Assoc. J.* **41**, 191–197.
- Ball, M. H. E., Marshall, I. A., Mitchell, J. P. and Rideal, G. (1989) An assessment of glass microspheres for use as number-based aerodynamic size standards. United Kingdom Atomic Energy Authority Internal Report AEEW-R2544, Atomic Energy Authority, U.K.
- Baron, P. A., Mazumder, M. K. and Cheng, Y. S. (1993) Direct-reading techniques using optical particle detection. In *Aerosol Measurement* (Edited by Willeke, K. and Baron, P. A.), pp. 381–409. Van Nostrand Reinhold, New York.
- Bartley, D. L., Chen, C.-C., Song, R. and Fischbach, T. J. (1994) Respirable aerosol sampler performance testing. *Am. Ind. Hyg. Assoc. J.* (in press).
- CEN (1993) Workplace atmospheres—size fraction definitions for measurements of airborne particles, EN481, CEN.
- Heitbrink, W. A. and Baron, P. A. (1992) An approach to evaluating and correcting aerodynamic particle sizer measurements for phantom particle count creation. *Am. Ind. Hyg. Assoc. J.* **53**, 427–431.
- Higgins, R. D. and Dewell, P. (1967) A gravimetric size-selecting personal dust sampler. In *Inhaled Particles and Vapours*, Vol. II (Edited by Davies, C. N.), pp. 575–586. Pergamon Press, Oxford.
- Iles, P. J. (1990) Size selection of fibres by cyclone and horizontal elutriator. *J. Aerosol Sci.* **21**, 745–760.
- Kenny, L. C. and Lidén, G. (1991) A technique for assessing size-selective dust samplers using the APS and polydisperse aerosols. *J. Aerosol Sci.* **22**, 91–100.

- Lidén, G. and Kenny, L. C. (1991) Comparison of measured respirable dust sampler penetration curves with sampling conventions. *Ann. occup. Hyg.* **35**, 485–504.
- Lidén, G. and Kenny, L. C. (1993) Optimisation of the performance of existing respirable dust samplers. *Appl. occup. environ. Hyg.* **8**, 386–391.
- Maguire, B. A., Barker, D. and Wake, D. (1973) Size-selection characteristics of the cyclone used in the SIMPEDS 70 MK 2 gravimetric dust sampler. *Staub* **33**, 95–98.
- Ogden, T. L., Barker, D. and Clayton, M. P. (1983) Flow dependence of the Casella respirable-dust cyclone. *Ann. occup. Hyg.* **27**, 261–271.
- Rader, D. J., Brockmann, J. E., Ceman, D. L. and Lucero, D. A. (1990) A method to employ the Aerodynamic Particle Sizer factory calibration under different operating conditions. *Aerosol Sci. Technol.* **13**, 514–521.
- Rader, D. J. and O'Hern, T. J. (1993) Optical direct-reading techniques: *in situ* sensing. In *Aerosol Measurement* (Edited by Willeke, K. and Baron, P. A.), pp. 345–380. Van Nostrand Reinhold, New York.
- TSI (1987) *Aerodynamic Particle Sizer Manual*, TSI Inc., U.S.A.
- Vaughan, N. P. (1983) Investigation of size fractionating sampler characteristics using a real-time aerodynamic particle sizer. HSE Internal Report IR/L/FD/83/9, Health and Safety Executive, U.K.
- Vincent, J. H. (1989) *Aerosol Sampling Science and Practice*. Wiley, Chichester.
- Wake, D. (1989) Anomalous effects in filter penetration measurements using the Aerodynamic Particle Sizer (APS3300). *J. Aerosol Sci.* **20**, 13–17.
- Wang, H.-C. and John, W. (1987) Particle density correction for the Aerodynamic Particle Sizer. *Aerosol Sci. Technol.* **6**, 191–198.